

Direct-Dynamics Approaches to Proton Tunneling Rate Constants. A Comparative Test for Molecular Inversions and an Application to 7-Azaindole Tautomerization

Antonio Fernández-Ramos,^{†,‡} Zorka Smedarchina,[†] Willem Siebrand,^{*,†} Marek Z. Zgierski,[†] and M. A. Rios[‡]

Contribution from the Steacie Institute for Molecular Sciences, National Research Council of Canada, Ottawa, K1A 0R6 Canada, Department of Physical Chemistry, Faculty of Chemistry, University of Santiago de Compostela, 15706 Santiago de Compostela, Spain

Received December 15, 1998. Revised Manuscript Received April 27, 1999

Abstract: Tunneling rate constants as a function of temperature are calculated for (a) three medium-size molecules undergoing inversion: oxiranyl, dioxolanyl, and aziridine, together with their monodeutero isotopomers, and (b) two larger species undergoing tautomerization: excited 7-azaindole and its 1:1 complex with water. The former calculations allow a comparison of two direct-dynamics methods for multidimensional tunneling: transition-state theory with semiclassical tunneling corrections (TST/ST) and the instanton approach. The latter calculations illustrate the possibility of applying the instanton approach to biological model systems. The potential-energy surfaces for the inversions are evaluated on the basis of density functional theory at the level (U)B3LYP/6-31G*, which for the present problem is shown to yield results similar to UQCISD/6-311+G**. All vibrational degrees of freedom are included in the calculations and, except for minor adjustments of barrier heights, all parameters are used as calculated. The TST/ST calculations are performed with the GAUSSRATE 7.2 program in the small-curvature approximation and the instanton calculations with the DOIT 1.1 program. For the same input parameters the two methods produce very similar results, which are in excellent agreement with the observed rate constants (except for the well-known artifact that leads GAUSSRATE to converge to the wrong low-temperature limit). These results clearly show that, even in the case of inversions characterized by low tunneling frequencies and barriers, tunneling dominates the dynamics well beyond room temperature, implying that for all reactions in which a proton is exchanged between two heavier atoms, tunneling transfer will tend to remain dominant at even higher temperatures. While both methods support this conclusion and are capable of yielding reliable tunneling rate constants, they differ greatly in efficiency, the instanton method being considerably faster and therefore able to deal with much larger systems. This is demonstrated on 7-azaindole, which, together with its 1:1 complex with water, has been used as a biological model system. Comparison of the calculated rate constants of tautomerization by proton transfer in the excited state with the available data sheds new light on the proposed transfer mechanism in protic solutions. The instanton calculations are based on the same method and program as those for the inversions, except for a lower level of quantum chemistry.

1. Introduction

Transfer of a hydrogen atom or a proton is a basic step in numerous chemical reactions. It is also implicated in many biological processes, where proton transfer is an alternative to electron transfer, operative on different time and distance scales. For instance, several enzymatic reactions show strong kinetic isotope effects,¹ indicating that hydrogen transfer is one of the rate determining steps. Another example is double proton transfer among DNA bases, which has been discussed as a mechanism for DNA mutation.² Also, the role of water in the transfer of amino acids to their zwitterionic form has been the subject of many studies.^{3–5} To unravel these complex processes, it is of great help to be able to calculate the rate of proton

transfer, since rate constants are observables and allow direct comparison with experiment. However, this has proved to be a nontrivial problem for these systems, since the transfer tends to be dominated by quantum-mechanical tunneling, a mechanism that allows protons to transfer efficiently at modest temperatures, even in the presence of relatively high energy barriers. The observed “activation energy” is temperature-dependent, generally much smaller than the barrier height, and actually goes to zero in the low-temperature limit. To deal quantitatively with the dynamics of reactions involving hydrogen transfer, one clearly has to come to terms with this nonclassical behavior.

This requirement has been a serious impediment to the quantitative prediction of proton transfer rate constants in systems too large to allow a full quantum-mechanical treatment. Most treatments of hydrogen transfer in large systems are limited to an evaluation of the properties of the energy barrier and do not address the actual tunneling dynamics, so that a direct comparison of theory and experiment is not possible. Of course it is well-known how to calculate the rate of tunneling through a one-dimensional barrier;⁶ this method is, in fact, widely used

[†] Steacie Institute for Molecular Sciences.

[‡] University of Santiago de Compostela.

(1) Kohen, A.; Klinman, J. P. *Acc. Chem. Res.* 1998, 31, 397.

(2) Ingham, K. C.; El-Bayoumi, M. A. *J. Am. Chem. Soc.* 1974, 96, 1674.

(3) Sheinblatt, M.; Gutowsky, H. S. *J. Am. Chem. Soc.* 1964, 86, 4814.

(4) Chang, K. C.; Grunwald, E. *J. Phys. Chem.* 1976, 80, 1422.

(5) Yensen, J. H.; Gordon, M. S. *J. Am. Chem. Soc.* 1995, 117, 8159.

to examine organic reaction mechanisms.⁷ However, proton tunneling can rarely be satisfactorily described as a one-dimensional process: Evidently the motion of the atoms between which the proton is being exchanged will have a major effect on the tunneling rate.^{8–14} This recognition has led to the introduction of two-dimensional approaches in which the second dimension represents the effective motion of the other atoms during the proton transfer.^{8,10,12,13,15,16} Although two-dimensional models have produced a great deal of qualitative insight into such phenomena as the kinetic isotope effect and the temperature dependence of the transfer process, they still require the introduction of empirical parameters and thus cannot give rise to quantitative predictions. For quantitative work it is necessary to consider *all* degrees of freedom of the system.

Obviously, this will be a daunting task for actual biological systems; one may reasonably expect, however, that much can be learned from the study of models that mimic their basic properties. The present paper is part of a project to develop a dynamics method that can deal quantitatively with proton transfer rates in such models. Following the introduction of a method based on instanton theory, it aims to probe the accuracy of this method by comparing its results not only with experimental data, where agreement might be fortuitous, but also with another, well-established theoretical method in a domain where this method has proved to be effective. Armed with these results, we then demonstrate that our method remains manageable well outside this small-systems domain and can probe the proposed hydrogen-transfer mechanism in a molecule of biological interest.

The standard approach to chemical reaction rates is transition-state theory,¹⁷ which is basically a statistical approach in which the rate constant is fully determined by the Gibbs free-energy difference between the transition state, identified as the top of the potential-energy barrier, and the equilibrium configuration. This theory allows one to go beyond low-dimensional models and to adopt a multidimensional approach in which all degrees of freedom of the system enter, namely through the partition functions of the equilibrium configuration and the transition state. The original formulation of transition state theory by Wigner¹⁸ is purely classical and involves the assumption that there is no recrossing of the barrier after the first passage. In variational transition-state theory (VTST), this assumption is mitigated by moving the dividing plane of the transition state to a position along the reaction coordinate where recrossing is minimized.¹⁹ In the quantum version of TST, the nonseparability

of the reaction coordinate from the transverse coordinates is addressed by allowing for coupling between them (e.g., see ref 20). Quantum-mechanical tunneling is included by the addition of semiclassical tunneling corrections, which leads to a version called TST/ST (or VTST/ST);¹⁹ for applications to actual systems, so-called direct-dynamics programs have been made available²¹ that allow one to derive the dynamics directly from the output of standard quantum-chemical codes. These programs come in two forms, called the small-curvature tunneling (SCT) and large-curvature tunneling (LCT) approximation, respectively, between which a choice must be made on a priori or a posteriori grounds. The SCT approximation^{22,23} is based on a tunneling trajectory derived from the minimum-energy path (MEP) through the inclusion of (weak) couplings of the tunneling mode to the transverse modes, which are treated adiabatically; such couplings reduce the effective mass of the tunneling particle and thus enhance the tunneling rate. The alternative LCT approximation²⁴ is indicated if there is strong coupling to the transverse modes and is based on an assumed straight-line tunneling trajectory connecting the regions of the two minima; since it is very demanding in computer time, few applications to large systems have been reported to date. Note that among all possible trajectories the MEP is the longest but has the lowest barrier, whereas the straight-line path represents the shortest trajectory with the highest barrier. In general neither of these trajectories is optimal. The best compromise at any given temperature is the trajectory that minimizes the classical action. Although direct search methods have been developed to find this trajectory,²⁵ they are even more demanding computationally than the LCT approximation and therefore limited to very small systems.

However, it has been found that the notion of an optimal tunneling trajectory governed by the minimum-action principle is a powerful concept in the theory of tunneling dynamics.²⁶ The corresponding theoretical framework is known as “instanton” theory (e.g., see refs 12 and 13 and references therein); formally the instanton path is defined as the trajectory that minimizes the classical action in the upside-down potential. We have recently shown^{27–35} that this concept remains fruitful even for systems for which an accurate evaluation of the instanton

(20) Pechukas, P. *Annu. Rev. Phys. Chem.* **1981**, 32, 159.

(21) GAUSSRATE 7.2, 1997, Corchado, J. C.; Coitino, E. L.; Chuang, Y.-Y.; Truhlar, D. G.; POLYRATE 7.2, 1997, Stecker, R.; Chuang, Y.-Y.; Coitino, E. L.; East, P. L.; Corchado, J. C.; Hu, W.-P.; Liu, Y.-P.; Lynch, G. C.; Nguyen, K.; Jackels, C. F.; Gu, M. Z.; Rossi, I.; Clayton, S.; Melissas, V.; Garrett, B. C.; Isaacson, A. D.; Truhlar, D. G.

(22) Miller, W. H.; Handy, N. C.; Adams, J. E. *J. Chem. Phys.* **1980**, 72, 99.

(23) Skodje, R. T.; Truhlar, D. G.; Garrett, B. C. *J. Phys. Chem.* **1981**, 85, 3019.

(24) Garrett, B. C.; Joseph, T.; Truong, T. N.; Truhlar, D. G. *Chem. Phys.* **1989**, 136, 271.

(25) Garrett, B. C.; Truhlar, D. G. *J. Chem. Phys.* **1983**, 79, 4931.

(26) Miller, W. H. *J. Chem. Phys.* **1975**, 62, 1899.

(27) Smedarchina, Z.; Siebrand, W.; Zgierski, M. Z.; Zerbetto, F. *J. Chem. Phys.* **1995**, 102, 7024.

(28) Smedarchina, Z.; Caminati, W.; Zerbetto, F. *Chem. Phys. Lett.* **1995**, 237, 279.

(29) Smedarchina, Z.; Siebrand, W.; Zgierski, M. Z. *J. Chem. Phys.* **1995**, 103, 5326.

(30) Smedarchina, Z.; Siebrand, W.; Zgierski, M. Z. *J. Chem. Phys.* **1996**, 104, 1203.

(31) Smedarchina, Z.; Fernández-Ramos, A.; Rios, M. A. *J. Chem. Phys.* **1997**, 106, 3956.

(32) Smedarchina, Z.; Zerbetto, F. *Chem. Phys. Lett.* **1997**, 271, 189.

(33) Fernández-Ramos, A.; Smedarchina, Z.; Zgierski, M. Z.; Siebrand, W. *J. Chem. Phys.* **1998**, 109, 1004.

(34) Smedarchina, Z.; Zgierski, M. Z.; Siebrand, W.; Kozłowski, P. M. *J. Chem. Phys.* **1998**, 109, 1014.

(35) Siebrand, W.; Smedarchina, Z.; Zgierski, M. Z.; Fernández-Ramos, A. *Int. Rev. Phys. Chem.* **1999**, 18, 1st issue.

(6) Bell, R. P. *The tunnel effect in chemistry*; Chapman and Hall: London, 1980.

(7) Melander, L.; Saunders, W. H. *Reaction Rates of Isotopic Molecules*, 2nd ed.; Wiley and Sons: 1980; pp 26–27, 42–44, 129, 174–176.

(8) Lippincott, E. R.; Schroeder, R. *J. Chem. Phys.* **1955**, 23, 1099, 1131.

(9) Bicerano, J.; Schaefer, H. F., III; Miller, W. H. *J. Am. Chem. Soc.* **1983**, 105, 2550.

(10) Siebrand, W.; Wildman, T. A.; Zgierski, M. Z. *J. Am. Chem. Soc.* **1984**, 106, 4083, 4089.

(11) Smedarchina, Z.; Siebrand, W. *Chem. Phys.* **1993**, 170, 347.

(12) Benderskii, V. A.; Goldanskii, V. I.; Makarov, D. E. *Phys. Reports* **1993**, 233, 195.

(13) Benderskii, V. A.; Makarov, D. E.; Wight, C. H. *Adv. Chem. Phys.* **1994**, 88, 1.

(14) Liu, Y.-P.; Lu, D.-h.; Gonzalez-Lafont, D. G.; Truhlar, D. G.; Garrett, B. C. *J. Am. Chem. Soc.* **1993**, 115, 7806.

(15) Smedarchina, Z.; Siebrand, W.; Zerbetto, F. *Chem. Phys.* **1989**, 136, 285.

(16) Bosch, E.; Moreno, M.; Lluch, J. M.; Bertran, J. *J. Chem. Phys.* **1990**, 93, 5685.

(17) Truhlar, D. G.; Garrett, B. C.; Klippenstein, S. J. *J. Phys. Chem.* **1996**, 100, 12771.

(18) Wigner, E. P. *Z. Trans. Faraday Soc.* **1938**, 34, 29.

(19) Truhlar, D. G.; Isaacson, A. D.; Garrett, B. C. *Theory of chemical reaction dynamics*; Baer, M., Ed.; CRC Press: Boca Raton, 1985; Vol. 4.

path is impractical. Starting from the instanton approach introduced by Miller²⁶ and further developed by Benderskii and co-workers,^{12,13} we have turned this approach into a powerful multidimensional alternative to TST/ST. Rather than attempt to calculate the instanton path directly, we have developed an approximation scheme that focuses on the corresponding instanton action, from which one can determine the rate constant as a function of temperature, its zero-temperature limit being related to the tunneling splitting of the ground-state energy level. In our approach the instanton action is numerically evaluated for the one-dimensional potential and then analytically corrected for coupling to transverse modes so as to yield simple expressions for tunneling rates and tunneling splittings. The direct-dynamics program DOIT (dynamics of instanton tunneling)³⁶ evaluates these expressions directly from calculated energies, structures, and vibrational force fields of the stationary configurations of the potential, which are the output of commonly used quantum-chemical software packages such as GAUSSIAN.³⁷

In its strict but, for large systems, unmanageable form, instanton theory is basically “exact” up to the crossover temperature $\omega^*/2\pi$, where ω^* denotes the imaginary frequency at the transition state. In the form used here³⁶ it involves a number of more or less severe approximations, made with the dual purpose of allowing a direct link with quantum-chemical programs and extending the usefulness of the method beyond the crossover temperature. As our reaction coordinate we choose not the MEP but the normal mode with imaginary frequency in the transition state; the transverse modes are the other normal modes of the transition state. The coupling of these modes to the reaction coordinate is assumed to be linear and derived from their displacement between the stationary points; this does not require the adiabatic approximation. Coupling between the transverse modes is neglected. In this lowest-order form of our method, the only quantum-chemical input data required are the structures, energies, and force fields of the stationary states, whereas the TST/ST method requires a large number of such calculations along the MEP and, in the LCT approximation, energy calculations along the straight path as well. As a result the computer time required for the evaluation of a set of rate constants by the instanton method is only a fraction of the time required by the TST/ST method. Since our method is very different from TST/ST, it is of interest to compare the two methods and to assess their areas of applicability. For the comparison we use versions of the two methods that are available in the form of readily accessible computer codes. In two earlier papers we have carried out such a comparison for tunneling splittings in glycolate anion³¹ and 9-hydroxyphenalene,³³ and found that the instanton method was not only much faster, as expected, but also more accurate. The instanton method accounted more accurately for the observed isotope effects and, in addition, it was able to account for splittings of vibrationally excited levels of low-frequency skeletal modes while TST/ST was not. In the present paper we compare the accuracy and efficiency of the two methods for the calculation of tunneling

rate constants. To this end we have chosen three medium-size molecules that undergo inversion. This test is less stringent than a test involving actual transfer of a hydrogen atom; however, molecules for which good hydrogen-transfer rate constants have been reported are for the moment too large for accurate calculations based on the TST/ST method.³⁸ The present molecules have the advantage that they are simple enough to allow an accurate evaluation of the potentials and force fields, so that a tripartite comparison is possible involving both dynamics methods and the available sets of experimental data. To compare the methods, we use the same level of quantum chemistry for both; where the agreement with experiment can be improved by minor adjustment of the calculated barrier height, the most critical parameter in the calculations, we again use the same correction for both methods.

The ultimate aim of this comparison is to establish the suitability of our method for the evaluation of hydrogen-transfer rate constants in model systems of biological interest. Such applications require not only calculation of rate constants but also a demonstration that the model used is relevant. The latter aspect will be left for a future publication; here we limit ourselves to an example that has received much attention as a model for DNA bases, namely 7-azaindole (e.g., see the recent review of Smirnov et al.³⁹), which can be optically excited to a metastable tautomer. For this excited state we calculate the rate of double proton transfer in its 1:1 complex with water as a function of temperature and isotopic substitution to demonstrate that the method can indeed deal with systems of biological interest. Three of the molecules to be considered have earlier served as examples in the first paper of our series on the instanton approach to hydrogen tunneling.²⁷ Since these results were reported, this approach has been applied to other systems and has undergone considerable development.^{28–38} Also, the earlier calculations were based incorrectly on the normal coordinates of the equilibrium configuration rather than on those of the transition state. In addition, facilities have become available that allow us to upgrade the level of the quantum-chemical calculations. This has made it possible to repeat our earlier calculations at a much improved level and compare the results with new TST/ST calculations performed at the same level.

The two direct-dynamics methods have been reviewed recently^{17,35} and will therefore be treated here in a simplified form. The TST/ST calculations are performed with the GAUSS-RATE 7.2 program²¹ and the instanton calculations with the DOIT 1.1 program.³⁶ For the required quantum-chemical input data, the GAUSSIAN 94 suite of programs³⁷ was used.

2. Outline of the Dynamics Procedures

We first give a short outline of the instanton approach developed in earlier studies; for more details see refs 12, 13, 33–35. In the instanton method the tunneling rate constant is calculated from

$$k(T) = (\Omega_0/2\pi)e^{-S_I(T)} \quad (1)$$

where Ω_0 is the effective tunneling mode frequency in the equilibrium configuration, obtained by a unitary transformation from the transition-state frequencies, and $S_I(T)$ is the instanton action (in units \hbar). Both of these quantities are derived from the full-dimensional potential-energy surface calculated by ab

(36) Smedarchina, Z.; Fernández-Ramos, A.; Zgierski, M. Z.; Siebrand, W. DOIT1.1, a computer program to calculate hydrogen tunneling rate constants and splittings, National Research Council of Canada, <http://www.sims.nrc.ca/sims/software/doit/index.html>.

(37) Gaussian 94, Revision B.3, Frisch, M. J.; Trucks, G. W.; Schlegel, H. B.; Gill, P. M. W.; Johnson, B. G.; Robb, M. A.; Cheeseman, J. R.; Keith, T.; Petersson, G. A.; Montgomery, J. A.; Raghavachari, K.; Al-Laham, M. A.; Zakrzewski, V. G.; Ortiz, J. V.; Foresman, J. B.; Peng, C. Y.; Ayala, P. Y.; Chen, W.; Wong, M. W.; Andres, J. L.; Replogle, E. S.; Gomperts, R.; Martin, R. L.; Fox, D. J.; Binkley, J. S.; Defrees, D. J.; Baker, J.; Stewart, J. P.; Head-Gordon, M.; Gonzalez, C.; Pople, J. A. Gaussian Inc., Pittsburgh, PA, 1995.

(38) Al-Soufi, W.; Grellmann, K. H.; Nickel, B. *J. Phys. Chem.* **1991**, *95*, 10503.

(39) Smirnov, A. V.; English, D. S.; Rich, R. L.; Lane, J.; Teyton, L.; Schvabacher, A. V.; Luo, S.; Thornburg, R. W.; Petrich, J. W. *J. Phys. Chem. B* **1997**, *101*, 2758.

initio methods. This potential is expressed in the normal coordinates $\{x, \mathbf{y}\}$ of the transition state, where x is the mode with imaginary frequency, taken to be the reaction coordinate. Displacements between the equilibrium configuration and the transition state, taken as origin, are denoted by Δx and $\Delta \mathbf{y}$. The transverse modes $\{\mathbf{y}\}$ are assumed to be harmonic with frequencies $\omega_{a,s}$, but no restriction is placed on the potential along the reaction coordinate x . This leads to an adiabatic potential of the form

$$U(x, \mathbf{y}) = U_A(x) + \frac{1}{2} \sum_s \omega_s^2 (y_s - x^2 C_s / \omega_s^2)^2 + \frac{1}{2} \sum_a \omega_a^2 (y_a \mp x C_a / \omega_a^2)^2 \quad (2)$$

where the subscript $a(s)$ refers to vibrations that are antisymmetric (symmetric) relative to the dividing plane of the transition state and the factors $C_{a,s}$ are linear couplings:

$$C_a = \omega_a^2 \Delta y_a / \Delta x, \quad C_s = \omega_s^2 \Delta y_s / \Delta x^2 \quad (3)$$

Since the inversion potentials are symmetric, these equations assume a very simple form; however, generalization to asymmetric potentials is straightforward.^{34,35}

We transform calculated atomic displacements \mathbf{r} between the transition state and the stable configuration into vibrational displacements through the relation $\Delta\{x, \mathbf{y}\} = \mathbf{r} \cdot \mathbf{L}$, where \mathbf{r} is the vector of the mass-weighted atomic displacements between the stationary configurations and \mathbf{L} is the $3N \times (3N - 6)$ matrix that relates $\{x, \mathbf{y}\}$ to the mass-weighted Cartesian coordinates of the atoms in the transition state. With these definitions, the instanton action assumes the form

$$S_1^0(T) = \frac{S_1^0(T)}{1 + \sum_s \delta_s(T)} + \alpha_s \sum_a \delta_a(T) \quad (4)$$

In this expression $S_1^0(T)$ is the one-dimensional instanton action along the reaction coordinate

$$S_1^0(T) = 2 \int_{x_1}^{x_2} \{2m_{\text{eff}}[U_A(x) - E^*(T)]\}^{1/2} dx \quad (5)$$

where $x_{1,2}$ are classical turning points for energy $E^*(T)$ where the period of the motion in the upside-down potential $-U_A(x)$ equals $\hbar/k_B T$. For numerical work it is more convenient, however, to calculate $S_1^0(T)$ from its relation through eq 1 to the standard semiclassical expression for the rate of one-dimensional tunneling

$$k^0 = Z_0^{-1} \int_{\hbar\Omega_0/2}^{U_0} P(E) e^{-E/k_B T} dE \quad (6)$$

where Z_0 is the one-dimensional partition function, $P(E)$ is the quasi-classical barrier penetration factor, and the integral runs from the effective zero-point energy level in the initial state to the top of the barrier. This extends the definition of $S_1^0(T)$ to regions beyond the crossover temperature $\omega^*/2\pi$. In these expressions the effective mass of the tunneling particle is given by

$$m_{\text{eff}} = 1 + \sum_a (C_a / \omega_a^2)^2 + 4x^2 \sum_s (C_s / \omega_s^2)^2 \quad (7)$$

where the summations are restricted to modes with a high frequency relative to the (imaginary) inversion frequency. The

lower-frequency transverse modes contribute via the correction terms $\delta_{a,s}$ in eq 4, which are expressed in terms of the linear couplings $C_{a,s}$ of eq 3 as detailed in refs 33–35. Note that the δ_a contribute effectively to the Franck–Condon factor of the transition and thus lower the rate, whereas the δ_s facilitate the transfer. The factor $\alpha_s \leq 1$ in eq 4 describes the modulation of the antisymmetric correction by the symmetric coupling.^{13,34}

The rate constant so defined comprises tunneling from levels above the zero-point level. Its contribution, which is to be added to the rate constant of eq 1, represents the zero-temperature limit of the rate constant, given by eqs 1 and 4 in the limit $T \rightarrow 0$, where $S_1^0(0) = 2S_C(\hbar\Omega_0/2)$, i.e., twice the classical action for the zero-point energy level. To evaluate the one-dimensional adiabatic barrier $U_A(x)$, we use the barrier height U_0 and the displacement Δx as (half) the barrier width, together with the calculated curvatures at the stationary configurations. By definition, the points at which $U_A(x)$ is evaluated must obey the conditions $\partial U(x, y_{a,s}) / \partial y_{a,s} = 0$ for all modes $y_{a,s}$, so that the gradient is directed along x . It is evident that points along the MEP do not obey these conditions, because our reaction coordinate is the mode with imaginary frequency in the transition state and, except in this point, does not coincide with the MEP. Since the curvatures at the stationary points are evaluated, the direction of this gradient is known near these points. Therefore, a simple way to approximate the potential $U_A(x)$ for intermediate points is to connect the regions of the stationary points by their common tangent, i.e., the tangent at the parabolas corresponding to the frequency ω^* of the transition state and Ω_0 of the equilibrium configuration. This procedure proved sufficient in the present paper and in all cases studied so far. If a more accurate potential is needed, it is necessary to find intermediate configurations that obey the above conditions and to determine their energy; this problem will be discussed elsewhere.

In transition-state theory tunneling corrections are introduced through a transmission factor $\kappa(T) > 1$ that scales the classical rate constant and is defined as the Boltzmann average of the ratio of the quantum and the classical probabilities. The quantum probability is evaluated semiclassically. If the tunneling path is close to the MEP, we can use Miller's reaction-path Hamiltonian²²

$$H(p_s, s, \mathbf{P}, \mathbf{Q}) = \sum_{k=1}^{3N-7} [1/2 P_k^2 + 1/2 \omega_k(s)^2 Q_k^2] + V_0(s) + \frac{1}{2} \frac{[p_s - \sum_{k,l=1}^{3N-7} Q_k P_l B_{k,l}(s)]^2}{[1 + \sum_{k=1}^{3N-7} Q_k B_{k,3N-6}(s)]^2} \quad (8)$$

where s is the MEP, taken as the reaction coordinate, p_s is its conjugate momentum, and $\mathbf{Q}(\mathbf{P})$ denote the $3N - 7$ transverse vibrational coordinates (momenta), which depend parametrically on s ; $V_0(s)$ represents the potential along s ; the parameters $B_{k,l}(s)$ represent couplings between the transverse modes, which are orthogonal to the reaction coordinate, each of which is coupled through $B_{k,3N-6}(s)$ to the reaction coordinate (mode $3N - 6$). In the small-curvature approximation, which was found to be appropriate in the case at hand, all of the couplings $B_{k,l}(s)$ are neglected, and only the couplings between the $3N - 7$ orthonormal modes and s are retained. The effect of these couplings is to generate a centrifugal force, so that the actual tunneling path does not pass through the transition state but "cuts the corner" so as to become shorter and more energetic.

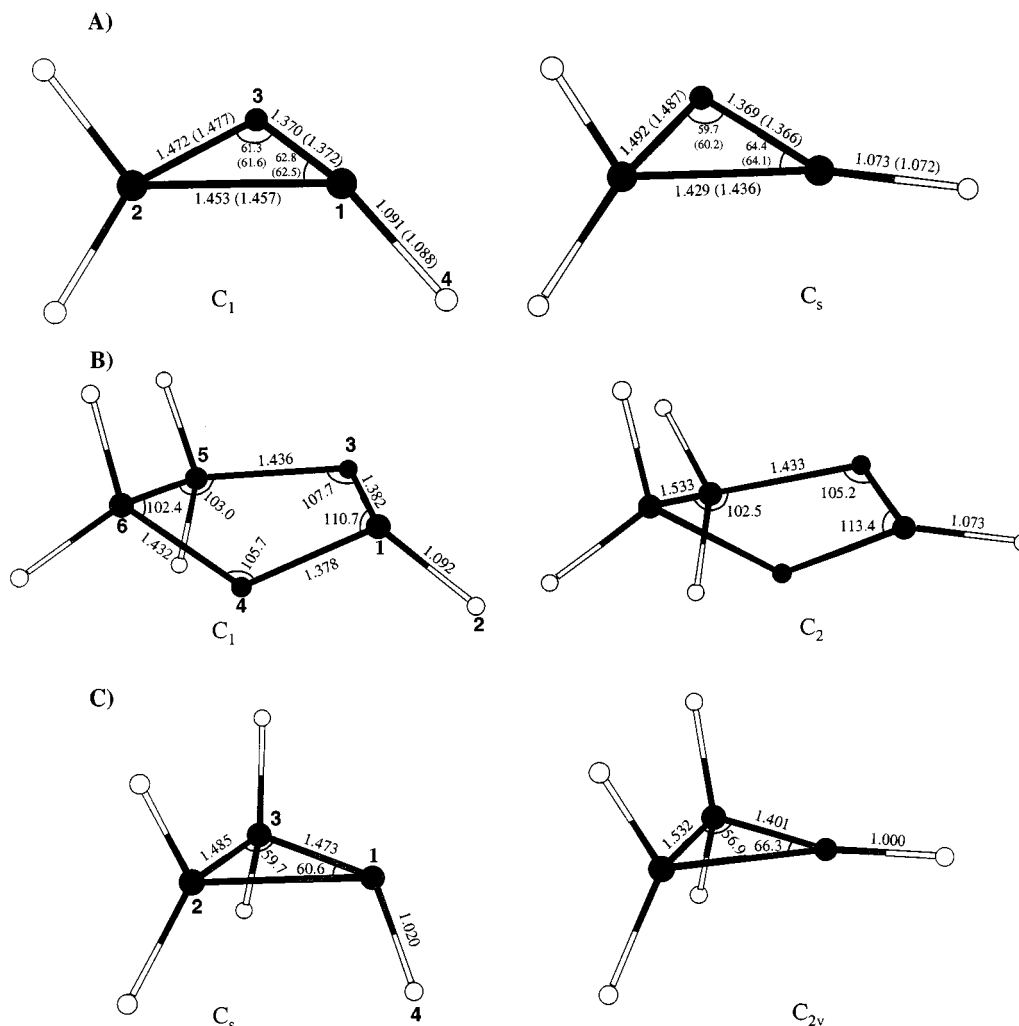


Figure 1. The equilibrium and transition-state configurations of (A) the oxiranyl radical, (B) the dioxolanyl radical, and (C) the aziridine molecule. Bond lengths are in Å, bond angles in degrees; numbers with and without brackets refer to (U)B3LYP/6-31G* and UQCISD/6-311+G** levels of calculation, respectively.

This introduces a factor smaller than unity in the denominator of the kinetic energy and thus has the same effect as decreasing the mass of the tunneling particle, namely to increase the inversion rate. It is obvious that the most favorable tunneling path will be a compromise between the shortest but most energetic path (the straight line connecting the minima) and the longest but least energetic path (the MEP); it is the path where the action is minimal. It was shown that the small-curvature path is the least-action path when the adiabatic approximation is valid for the transverse modes, i.e., when the coupled modes have a high frequency relative to the tunneling mode, as is the case for the molecules under consideration.⁴⁰ Only in that case can Miller's Hamiltonian be reduced to a quasi-one-dimensional form. In the opposite case, when the tunneling mode has the highest frequency, as in the case of transfer of a proton between two heavier atoms, the large-curvature path is relevant, which is very different from the MEP. Unfortunately, tunneling calculations based on this path require the evaluation of energies, gradients, and Hessians along the MEP, together with energy calculations along straight paths where the adiabatic approximation is not valid. This makes the LCT method computationally demanding for small molecules and impractical for large molecules, unless low-level electronic structure calculations are used.

3. Quantum-Chemical Calculations

Our earlier calculation of the tunneling potential and force field of the three molecules subject to inversion was carried out at the UHF/6-31G** level.²⁷ Comparison with observed tunneling rates indicated that at this level the inversion barrier is substantially overestimated and requires empirical correction. Following recent work at the UMP2 level by Barone et al.⁴¹ on cyclopropyl and oxiranyl radicals, we investigated a number of alternative schemes, using oxiranyl as an example. We extended the basis set to 6-311+G** after establishing that the inclusion of additional polarized orbitals yielded no further reduction of the barrier height. To improve on the perturbational UMP2 method, we used the variational UQCISD method, which further increased the barrier by 0.6 kcal/mol. Single-point calculations with triple excitations of the form UQCISD(T) did not produce a significant improvement. We also tried DFT and found that UB3LYP/6-31G* leads to essentially the same results as UQCISD/6-311+G**, not only for the barrier height but also for the structure, at a fraction of the cost in computer time. A summary of the results is listed in Table 1, where the structure is represented by the pyramidalization angle θ calculated as the projection of the CH bond on the plane of the atoms 1–3 depicted in Figure 1A, this angle being a measure of the

(40) Marcus, R. A.; Coltrin, M. E. *J. Chem. Phys.* **1977**, *67*, 2609.

(41) Barone, V.; Adamo, C.; Brunel, Y.; Subra, R. *J. Chem. Phys.* **1996**, *105*, 3168.

Table 1. Comparison of Tunneling Parameters for the Inversion of the Oxiranyl Radical Produced by Different Methods; the DFT Tunneling Parameters Are Listed also for the Dioxolanyl Radical and Aziridine

method	barrier height, U_{ad}^0 , kcal/mol	θ , deg
UHF/6-31G** ^a	9.0	56.5
UMP2/TZ2P ^b	8.3	46.0
UMP2/6-31G** ^c	7.6	45.2
UMP2/6-31+G** ^c	7.0	44.7
UMP2/6-311+G** ^c	6.6	44.5
UQCISD/6-311+G** ^c	7.2	44.9
UQCISD(T)/UQCISD/6-311+G** ^c	7.1	44.9
UB3LYP/6-31G** ^c	7.2	45.3
(dioxolanyl radical) UB3LYP/6-31G** ^c	5.9	43.2
(aziridine) B3LYP/6-31G** ^c	17.7	66.8 (63.3 ^d)

^a Reference 45. ^b Reference 41. ^c This study. ^d Experiment, ref 46.

tunneling path length. As expected, the barrier height increases with the pyramidalization angle in the order dioxolanyl, oxiranyl, aziridine. Since the transformation from the equilibrium configuration to the transition state changes the orbital character of the inversion center from sp^3 to sp^2 , there is an increase in π -bonding, which leads to the tightening of the ring structures shown in Figure 1.

To provide a meaningful comparison of the two methods, it is of course necessary to use the same level of quantum chemistry for both. Since the TST/ST method is far more demanding computationally than the instanton method, it determines the highest level of theory that is practical. In the present case this has led to the choice of the UB3LYP/6-31G* level for all three systems, following a detailed comparison of this level with the UQCISD/6-311+G** level for oxiranyl.

Our calculations on 7-azaindole and its 1:1 complex with water focus on the first excited singlet state, since this is the only state for which some kinetic data are available. The transfer barrier for the isolated molecule is calculated to be 67.2 kcal/mol at CIS/6-31G** level. As earlier deduced by Gordon,⁴² the imaginary frequency in the transition state of the complex corresponds to synchronous double proton transfer; the CIS/6-31G** calculations result in an adiabatic barrier of 25.2 kcal/mol. Since our earlier experiences indicate that this basis set tends to yield weak hydrogen bonds, we have repeated the calculation with the simple 3-21G basis set, which has been claimed⁴³ to give better hydrogen-bond parameters. The result is a barrier height of 11.1 kcal/mol as well as significantly shorter hydrogen bonds. Very recently, Chaban and Gordon⁴⁴ reported an adiabatic barrier height of 18.2 kcal/mol obtained at the MCSCF(10,9)/DZP level, which was reduced to 9.8 kcal/mol by single-point MCSCF-PT2 calculations. As our CIS calculations confirm, such a drastic reduction of the barrier is expected to be accompanied by a significant change in geometry, an issue not addressed by single-point calculations. These results thus suggest that the level of calculation achieved thus far is not yet sufficient to produce a reliable potential-energy surface for the complex. This means that dynamics calculations will produce relative rather than absolute rate constants.

4. Oxiranyl

The inversion rate constants of oxiranyl and its monodeutero isotopomer have been measured by modeling the temperature

Table 2. Absolute Values of the Displacements Δ (in $\text{\AA} \text{amu}^{1/2}$) between the Stable and Transition-State Structures of Oxiranyl- d_0 / $-d_1$, Obtained at the UQCISD/6-311+G** and UB3LYP/6-31G* Levels and Expressed in Terms of the Transition-State Symmetric and Antisymmetric Modes

UQCISD/6-311+G**		UB3LYP/6-31G*	
ω , cm^{-1}	Δ	ω , cm^{-1}	Δ
Symmetric Modes			
3386/2524	0.232/0.260	3375/2515	0.235/0.262
3124/3124	0.001/0.013	3091/3091	0.002/0.012
1556/1551	0.006/0.024	1558/1554	0.005/0.024
1383/1341	0.030/0.099	1389/1348	0.034/0.105
1224/1213	0.043/0.049	1216/1203	0.049/0.050
1108/1062	0.034/0.020	1089/1054	0.033/0.022
960/818	0.023/0.037	951/804	0.015/0.033
750/690	0.029/0.036	736/677	0.033/0.028
Antisymmetric Modes			
3211/3211	0.000/0.001	3168/3168	0.000/0.001
1102/1102	0.025/0.029	1095/1094	0.030/0.030
981/975	0.079/0.105	958/952	0.076/0.103
Reaction Coordinate			
885i/695i	0.693/0.901	864i/679i	0.699/0.909

dependence of their magnetic resonance spectrum.⁴⁵ At the low end of the temperature range 100–225 K, the spectrum of the undeuterated radical becomes temperature independent, the inversion being slow on the time scale of the experiment, while at the high end the spectra of both isotopomers tend toward a planar, averaged structure. The calculated barrier heights obtained at various levels of theory are listed in Table 1, as discussed in the preceding section. The normal-mode frequencies and displacements calculated at the UB3LYP/6-31G* and UQCISD/6-311+G** levels are compared in Table 2. The results are very similar, and the small differences have no significant effect on the proposed comparison of the two dynamics methods.

For the TST/ST calculations, the MEP was computed according to the Page–McIver procedure⁴⁷ with a step size of 0.01 bohr \cdot amu^{1/2}; the Hessians calculated at 0.05 and 0.1 bohr \cdot amu^{1/2} intervals produced the same absolute rate constants, indicating that the latter interval suffices. No scaling factors were used. In both methods the only transverse mode that is strongly coupled to the reaction coordinate is the CH-stretching mode of the tunneling proton. In the TST/ST method this mode shows a relatively large frequency change along the MEP as well as a substantial projection on the mode with imaginary frequency in the transition state. This implies that the tunneling path is shorter than the MEP. Since the CH-stretching mode has a much higher frequency than the inversion mode, its effect on the tunneling can be incorporated by a reduction of the effective mass of the tunneling particle. It turns out that the effect of this coupling on the tunneling rate is small; in other words, the tunneling trajectory stays close to the MEP, which represents zero-curvature tunneling. The tunneling being effectively one-dimensional in this case, the LCT and SCT approximations give basically the same tunneling rates.

In the instanton method the CH-stretching mode shows a large displacement. As in the TST/ST case, this coupling effect can be incorporated by a change in effective mass, which in this approach is an increase rather than a decrease, however, namely by a factor $1 + 0.94x^2$ ($1 + 0.42x^2$ for the D-substituted radical); the effect of this coupling on the rate is again small. Contrary

(42) Gordon, M. S. *J. Phys. Chem.* **1996**, *100*, 3974.

(43) Rios, M. A.; Rodríguez, J. *J. Comput. Chem.* **1992**, *13*, 860. Rodríguez, J. *J. Comput. Chem.* **1994**, *15*, 183.

(44) Chaban, G. M.; Gordon, M. S. *J. Phys. Chem. A* **1999**, *103*, 185.

(45) Deycart, S.; Luszyk, J.; Ingold, K. U.; Zerbetto, F.; Zgierski, M. Z.; Siebrand, W. *J. Am. Chem. Soc.* **1988**, *110*, 6721.

(46) Bak, B.; Skaarup, S. *J. Mol. Struct.* **1971**, *67*, 2609.

(47) Page, M., Jr.; McIver, J. W. *J. Chem. Phys.* **1987**, *88*, 922.

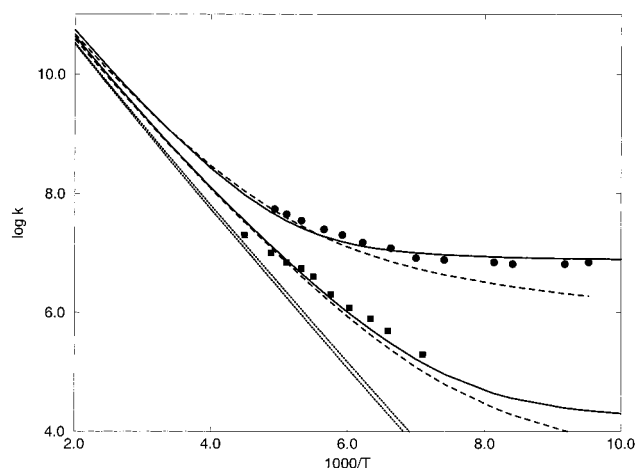


Figure 2. Comparison of observed and calculated absolute rate constants for the inversion of oxiranyl. The data (circles for oxiranyl- d_0 , squares for oxiranyl- d_1) are taken from ref 45; the solid and dashed lines represent calculated instanton and TST/SCT rate constants, respectively. The dotted lines represent the classical contributions.

to our earlier results, no other couplings are significant, so that the tunneling is effectively one-dimensional. The reason the effective-mass effect has the opposite sign in the two methods is that these methods start from different trajectories: the TST/ST method starts from a trajectory that is too long, namely the MEP, while the instanton method starts from a trajectory that is too short, namely the straight path corresponding to the inversion mode.

The quantum-chemical input data allow us to reproduce the observed inversion rate constants, provided we adjust the calculated barrier height by a factor 0.95 to 6.8 kcal/mol for both methods. With this adjustment, the agreement with the observed rate constants of both isotopomers is very satisfactory, as shown in Figure 2, where the solid lines represent the instanton results and the broken lines the TST/SCT results calculated with the same parameters. The two results are very similar, except near the low-temperature limit. GAUSSRATE does not converge to the correct low-temperature limit, since it computes the tunneling correction as a continuous Boltzmann average over energies in the initial configuration instead of as a discrete sum over energy levels. This approximation is not difficult to correct,⁴⁸ but this correction is not used here since it is not implemented in the program. The calculations also allow us to assess the relative contributions of classical and quantum transitions to the transfer process. The classical contributions follow the Arrhenius law and are represented by a dotted line for the light (top) and D-substituted (bottom) isotopomers. Comparison of the classical results with the total inversion rate constants calculated by the instanton and TST/ST methods shows that for undeuterated oxiranyl, tunneling transfer is dominant, i.e., the total rate constant is more than double the classical rate constant below 400 K; for the monodeuterio compound tunneling dominates below 250 K. The crossover temperatures of the instanton method for the two isotopomers are 200 and 155 K, respectively; Figure 2 shows that the instanton results remain consistent with the TST/SCT results above these temperatures and extrapolate smoothly to the classical limit. As explained in section 2, this is due to our method of evaluating the one-dimensional instanton action, which extends its definition to arbitrary temperatures.

(48) Lauderdale, J. G.; Truhlar, D. G. *J. Am. Chem. Soc.* **1985**, *107*, 4590.

Table 3. Same as Table 2 for Dioxolanyl- d_0 - d_1 , at UB3LYP/6-31G* Level

ω , cm^{-1}	Δ
Symmetric Modes	
3369/2496	0.132/0.166
3136/3136	0.000/0.002
3030/3030	0.003/0.004
1540/1540	0.002/0.004
1391/1392	0.001/0.000
1264/1263	0.015/0.018
1195/1172	0.018/0.044
1158/1156	0.016/0.034
994/984	0.016/0.041
946/946	0.001/0.001
764/758	0.084/0.065
247/247	0.194/0.194
Antisymmetric Modes	
3142/3142	0.000/0.000
3041/3041	0.002/0.001
1535/1535	0.001/0.001
1420/1404	0.005/0.004
1290/1249	0.008/0.008
1216/1194	0.001/0.003
1152/1059	0.003/0.000
1004/927	0.002/0.005
880/805	0.006/0.010
652/650	0.005/0.009
161/145	0.165/0.022

5. Dioxolanyl

The dioxolanyl radical, also depicted in Figure 1, has a rate of inversion that is too high to be measured by electron-spin resonance, unless it is deuterated at the carbon atom carrying the unpaired electron. The inversion rate constant of the monodeuterio isotopomer has been measured for temperatures covering a range from 100 to 190 K, running from temperature-independent to thermally activated inversion.⁴⁹ Our earlier attempt to calculate the observed rate constants led to the conclusion that anharmonic coupling terms were necessary to arrive at a satisfactory reproduction of the experimental data. The improved calculations, based on UB3LYP/6-31G*-level computations of the barrier height, structures, and force fields, as well as on a refined instanton approach, show that this conclusion was not justified. The recalculated normal-mode frequencies and displacements are listed in Table 3; they confirm the coupling to a symmetric ring-bending mode of 247 cm^{-1} , but this coupling is too weak to affect the rate constants substantially, leading effectively to a two-dimensional tunneling potential. In addition, there is coupling to the symmetric CH-stretch mode (although weaker than in the case of oxiranyl), which is included through mass-renormalization. The rate constants for the calculated barrier height of 5.9 kcal/mol are displayed in Figure 3, where the instanton results are shown as solid lines and the TST/SCT results as broken lines. Excellent agreement with experiment is obtained. Again the two methods yield very similar results except for those near the low-temperature limit, where the TST/SCT results are low, not only for the D-substituted isotopomer but also for the parent compound, since this method predicts values within the EPR detection range, contrary to what is observed.⁴⁹ As pointed out, this can be corrected by replacing the integral over tunneling energies by a summation over discrete levels. The classical results represented by dotted lines clearly indicate that tunneling dominates the inversion process in the temperature range studied experimentally. The crossover temperatures for dioxolanyl and

(49) Deycart, S.; Luszyk, J.; Ingold, K. U.; Zerbetto, F.; Zgierski, M. Z.; Siebrand, W. *J. Am. Chem. Soc.* **1990**, *112*, 4284.

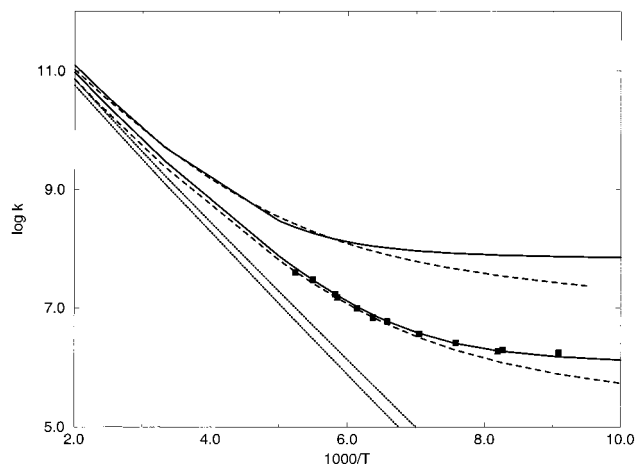


Figure 3. Same as Figure 2 but for the dioxolanyl radical. The experimental data are taken from ref 49.

Table 4. Same as Table 3 for Aziridine- d_0 - d_1

ω , cm^{-1}	Δ
Symmetric Modes	
3753/2762	0.500/0.611
3044/3044	0.023/0.006
3033/3034	0.000/0.000
1591/1589	0.042/0.005
1544/1544	0.000/0.000
1355/1331	0.028/0.083
1164/1150	0.000/0.000
1138/1129	0.000/0.105
1129/1118	0.126/0.000
974/850	0.000/0.101
856/746	0.168/0.000
Antisymmetric Modes	
3104/3104	0.001/0.004
3090/3090	0.000/0.000
1191/1180	0.081/0.108
1162/1162	0.000/0.000
1040/1040	0.000/0.000
864/858	0.080/0.129
Reaction Coordinate	
911i/710i	0.884/1.185

its monodeutero isotopomer are 200 and 165 K, respectively. It follows from Figure 3 that, as in the case of oxiranyl, the instanton results for the heavier isotopomer remain in agreement with experiment above the crossover temperature.

6. Aziridine

The inversion of the aziridine molecule has been studied by nuclear magnetic resonance in the gas phase at relatively high temperatures.^{50,51} Because these temperatures are well above the crossover temperatures, which for aziridine- d_0 and - d_1 were calculated to be about 210 and 165 K, respectively, this system provides an experimental test for the instanton approach. The two sets of experimental data that are available do not agree very well, and only one of them covers the deuterium isotope effect. The frequencies and displacements recalculated at the level B3LYP/6-31G* and displayed in Table 4 confirm the earlier conclusion that the only transverse mode that is strongly coupled to the inversion mode is the NH-stretching mode. Because of its high frequency, it can be treated in the adiabatic approximation. As a result, the inversion potential is basically

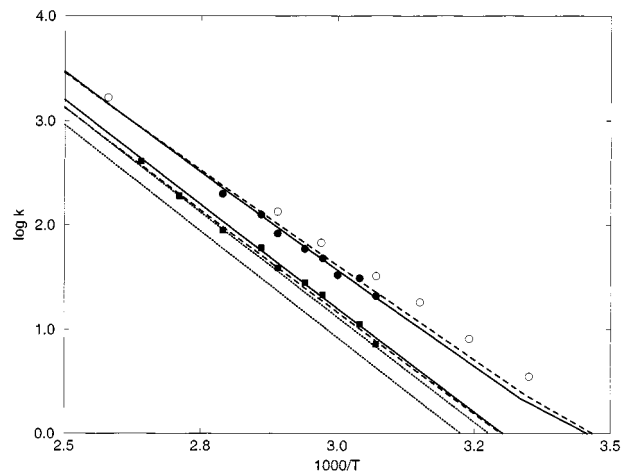


Figure 4. Same as Figure 2 but for the aziridine molecule. The experimental data are taken from ref 50 (open symbols) and from ref 51 (closed symbols).

one-dimensional, similar to that for oxiranyl. It turns out that both theories produce essentially the same results, which in Figure 4 are compared with the experimental data and with the classical results. It is concluded that for aziridine, but not for its N-deuterated isotopomer, tunneling remains the dominant inversion mechanism within the range of temperatures investigated, namely 325–380 K, but that classical transfer is beginning to contribute comparably near the upper part of this range. It is also clear that the validity of the instanton results is not limited to the region below the crossover temperature. The calculated results displayed in Figure 4 are based on a barrier adjusted for both methods by a factor 1.07 to a value of 19.0 kcal/mol; because of experimental uncertainties, it is difficult to judge the quality of the fit. We note that this correction brings the barrier in line with a very recent classical trajectory calculation with one-dimensional WKB tunneling corrections;⁵² it used a barrier height of 19.2 kcal/mol, calculated at the level MP2/6-311G(2df,2p) and resulted in a similar fit to the experimental data.

7. Application to 7-Azaindole

Having established that the instanton method yields reliable rate constants for inversion via hydrogen tunneling and accounts satisfactorily for the temperature and isotope dependence of porphine tautomerization,³⁴ we now apply the method to the molecule 7-azaindole, which has received much recent attention as a biological model system (e.g., see refs 39 and 53 and references therein). This molecule, depicted in Figure 5, exists in two tautomeric forms, such that the form that is stable in the ground state is metastable in the first excited state. Following optical excitation its dimer undergoes rapid tautomerization; because of this property it has been used as a model for DNA-base mutation.² The isolated monomer does not tautomerize within the lifetime of the fluorescence (5.7 ns⁵⁴), which is not surprising since the transfer barrier is calculated to be of the order of 60 kcal/mol. However, it tautomerizes rapidly in protic solvents, including water, presumably due to the formation of complexes such as 7-azaindole·H₂O, also depicted in Figure 5. Quantum-chemical calculations⁴² indicate that the tautomerization occurs by synchronous double proton transfer. The barrier

(52) Guo, Y.; Wilson, A. K.; Chabalowski, C. F.; Thompson, D. L. *J. Chem. Phys.* **1998**, *109*, 9258.

(53) Mente, S.; Maroncelli, M. *J. Phys. Chem. A* **1998**, *102*, 3860.

(54) Huang, Y.; Arnold, S.; Sulkes, M. *J. Phys. Chem. A* **1996**, *100*, 4734.

(50) Borchardt, D. B.; Bauer, S. H. *J. Chem. Phys.* **1986**, *85*, 4980.

(51) Carter, R. E.; Drakenberg, T.; N. A. Bergman, N. A. *J. Am. Chem. Soc.* **1975**, *97*, 6990.

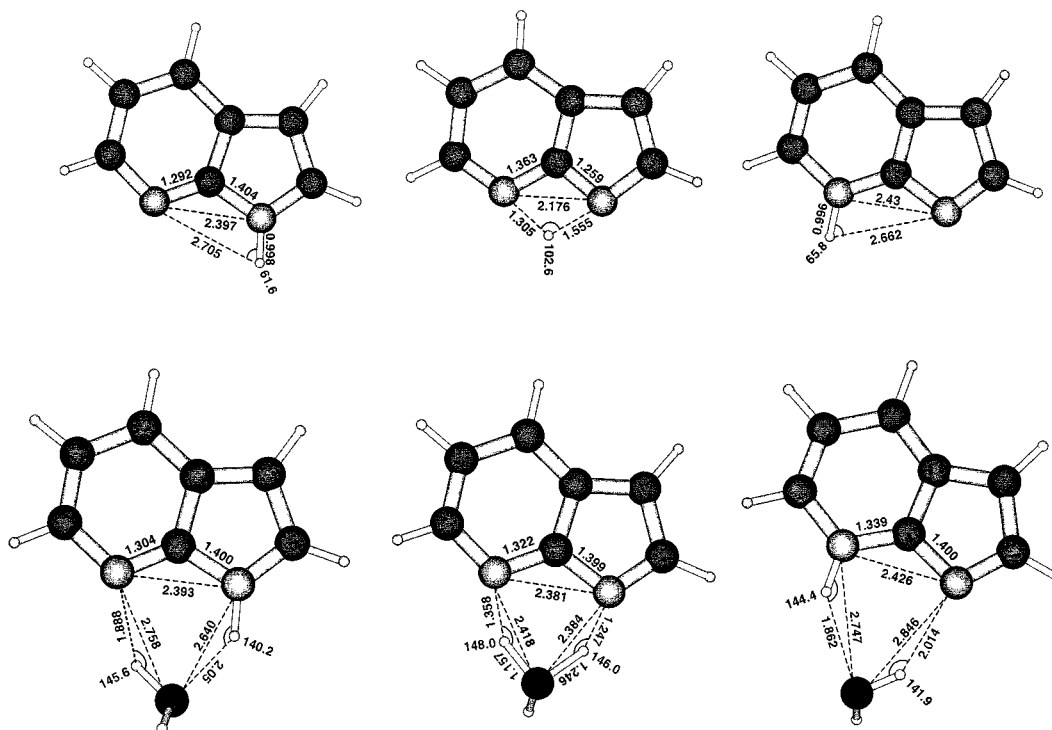


Figure 5. Structures of excited 7-azaindole in the initial, transition, and final state, respectively, calculated at the CIS/3-21G level, together with the corresponding structures of excited 7-azaindole·H₂O.

for this process is much lower than the barrier for tautomerization in the isolated molecule, but there have been no attempts to calculate transfer rate constants in these systems.

Cold-beam experiments show that the excited complex does not tautomerize within its fluorescence lifetime either. Note that this lifetime of 8.1 ns⁵⁴ exceeds the fluorescence lifetime of the isolated molecule, in qualitative agreement with calculations at the CIS/6-31G** level. The lack of observable tautomerization implies a transfer rate constant of the order of 10⁷ s⁻¹ or smaller. To relate this result to the quantum-chemical calculations, discussed in section 3, we need a method that allows us to calculate the corresponding rate constants. This can be readily accomplished by our program once a reliable potential-energy surface is obtained, but this is clearly not yet the case. However, our method allows us to reverse the problem and solve for the barrier height required to account for a given rate constant, starting from a calculated set of geometries and force fields. To account for the absence of tautomerization within the fluorescence lifetime, we find that the barrier must be at least 14 kcal/mol. Remarkably, this value is obtained for both the 3-21G and the 6-31G** structures and force fields, the former requiring an upward, the latter a downward, correction of the barrier. Obviously, it is very useful to have a method that can establish whether a given potential is compatible with observed rate constants.

To show that the method can also probe proposed reaction mechanisms, we plot in Figure 6 the calculated rate constants for double proton and double deuteron transfer in the excited complex as a function of temperature. The results are based on a barrier height adjusted to 14.0 kcal/mol in order not to contradict the cold-beam observations. Since the correction to the barrier height is smallest for the 3-21G basis set, we have used these results in the calculations; results based on the 6-31G** basis set are quite similar, however. The calculated kinetic isotope effect is typical for tunneling transfer. As further evidence that the transfer proceeds by tunneling, we also plot

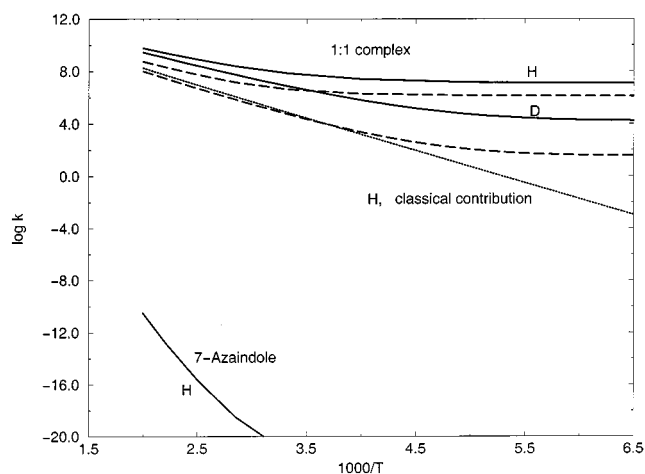


Figure 6. Tautomerization rate constants of 7-azaindole (bottom), 7-azaindole·H₂O (solid line, top), and N-deuterated 7-azaindole·D₂O (solid line, middle) calculated at the CIS/3-21G level with the barrier height adjusted to 14.0 kcal/mol. The broken lines indicate results obtained with the coupling to the transverse modes neglected and the dotted line represents classical results for the undeuterated complex.

the calculated classical transfer rate constants. It is interesting to consider the role of couplings to transverse modes. Their effect, which is dominated by symmetric low-frequency solvent-bridge modes, increases the calculated rate constants and reduces the isotope effect as illustrated in Figure 6. The calculated temperature dependence is weak, as expected for a tunneling reaction driven by a thermal energy much smaller than the barrier height, and cannot account for the fast tautomerization observed in protic solvents. This is not surprising: it indicates that the role of the solvent cannot be reduced to that of a simple proton bridge. Thus, the calculations indicate that the actual mechanism of 7-azaindole tautomerization in protic solvents remains to be explained. The same applies, ipso facto, for the

mechanism of tautomerization of guanine and of the DNA bases in general,⁵⁵ a problem that will be addressed elsewhere.

8. Discussion

The most striking result of the present investigation is the high level of agreement, not only between the two methods being compared but also between theory and experiment. The only clear discrepancy is the underestimation of the tunneling rate and the kinetic isotope effect in the low-temperature range by the GAUSSRATE program. This is an artifact that can be readily removed;^{48,56,57} however, in the context of the present work, we have used the available software in the form in which it is presented. The agreement shows clearly that hydrogen tunneling is not a low-temperature phenomenon that can be ignored at room temperature, even for simple inversions characterized by low tunneling frequencies and modest barriers. In the more important case of proton transfer between two heavier atoms, tunneling should remain the dominant transfer mechanism for much higher temperatures. Unfortunately, we have not been able to find systems of this kind that could be tested by the methods used for the inversions. The few systems for which adequate kinetic data are available are too large to be treated by the TST/LCT approximation indicated for such transfer. The largest systems treated thus far by this method are carboxylic acid dimers,⁵⁸ for which, however, few experimental data have been reported.

Although initially the instanton method was specially designed to deal with processes in the tunneling region, i.e., below the crossover temperature, in our formulation its validity is extended to arbitrary temperatures, and the results converge to the standard classical rate constant. Reduced to its bare essentials our method amounts to the following simple procedure: (1) calculate the rate constant for one-dimensional tunneling from eq 6, with zero-point corrections applied to the barrier height and with an effective mass that accounts for adiabatic coupling to high-frequency modes, (2) extract the corresponding one-dimensional instanton action by means of eq 1 and divide it by a factor

$$1 + \sum_s \delta_s$$

calculated from the displacements of symmetric transverse modes between the equilibrium configuration and the transition state, (3) multiply the resulting rate constant by a vibrational overlap integral derived from the corresponding displacements of antisymmetric modes, and (4) add the zero-temperature rate constant, which constitutes the contribution of the zero-point level, and the standard classical rate constant. Such a scheme is easy to apply even to very large systems, provided reasonably accurate quantum-chemical parameters can be obtained for the stationary points of the potential.

This opens the possibility of adding the calculation of rate constants to the arsenal of methods available to deal with

biological processes. These processes take place in an aqueous environment and involve molecules and polymers that abound in hydrogen bridges. Many of them involve transfer of a proton across such a bridge as an elementary step, although the detailed reaction mechanism is often not known. The pathway of a complex reaction is frequently determined by competition between such elementary steps; for instance, deuterium substitution at a critical site may alter the reaction path. The presence of water molecules is an important factor in these processes since they can participate directly in the transfer. It is therefore of great importance to develop a clear understanding of the rates of hydrogen tunneling reactions through a quantitative interpretation of experimental observations in quantum-mechanical terms.

The example of 7-azaindole illustrates several of these aspects. It shows the catalytic effect of a water bridge on proton transfer and it demonstrates the efficiency of coherent double proton transfer in hydrogen-bonded chains. Since rate constants, as opposed to barrier heights, are observables and allow direct comparison with experimental data, it was possible to show that this hydrogen bridge by itself is not sufficient to account for the rapid tautomerization of 7-azaindole observed in protic solvents. This followed from the absence of tautomerization in a cold beam within the fluorescence lifetime, combined with the weak temperature dependence deduced for the tunneling reaction. Clearly, model studies involving more solvent molecules are needed before we can reach a basic understanding of this process. Although in the present investigation the TST/ST and instanton methods produce comparable results for inversion reactions, in practical terms the corresponding programs are not equivalent since they differ greatly in the amount of computer time required. Although efforts have been announced to improve the computational efficiency of the TST/ST method,⁵⁹ at the present time the instanton method is much faster. Since the total time depends on the level of quantum-chemistry used, it is difficult to make exact comparisons. For the instanton method it is usually sufficient to calculate the geometry, energy, and force field at three stationary points of the surface. The amount of computer time required for the actual dynamics calculations is negligible. For the TST/ST method it is generally necessary to perform similar calculations at many points along the MEP and, in the large-curvature approximation, to perform additional energy calculations along the straight-line path. If the number of points required is $3 + n$, the instanton method is roughly $1 + n/3$ times faster than the TST/ST method; in practice this means that the systems that can be handled are larger by a factor of 10. This brings model systems of biological interest within the range of proton-transfer rate constant calculations, as the example of the 7-azaindole complex with water illustrates.

Acknowledgment. The paper, issued as NRCC No. 42180, is dedicated to Dr. Keith Ingold on the occasion of his 70th birthday. A.F.-R. thanks the Xunta de Galicia for financial support (Project XUGA20903A98). Z.S. thanks the University of Santiago de Compostela, Spain for hospitality during the visit in 1998 when this work was initiated.

JA984338T

(55) Watson, J. D.; Crick, F. H. C. *Nature* **1953**, *171*, 964. Topal, M. D.; Fresco, J. R. *Nature* **1976**, *263*, 285.

(56) Takayanagi, T.; Masaki, N.; Nakamura, K.; Okamoto, M.; Sato, S.; Schatz, G. C. *J. Chem. Phys.* **1987**, *86*, 6133.

(57) Hancock, G. C.; Mead, C. A.; Truhlar, D. G.; Varandas, A. J. C. *J. Chem. Phys.* **1989**, *91*, 3492.

(58) Loering, T.; Liedl, K. R.; Rode, B. M. *J. Am. Chem. Soc.* **1998**, *120*, 404. Loering, T.; Liedl, K. R. *J. Am. Chem. Soc.* **1998**, *120*, 12595.

(59) Chuang, Y.-Y.; Truhlar, D. G. *J. Phys. Chem. A* **1997**, *101*, 3808. Fast, P. L. *J. Chem. Phys.* **1998**, *109*, 3721. Corchado, J. C.; Coitiño, E. L.; Chuang, Y.-Y.; Fast, P. L.; Truhlar, D. G. *J. Phys. Chem. A* **1998**, *102*, 2424. Chuang, Y.-Y.; Corchado, J. C.; Truhlar, D. G. *J. Phys. Chem. A* **1999**, *103*, 1140.